Dielectric and conduction effects in non-Ohmic electrorheological fluids

C. W. Wu* and H. Conrad
Department of Materials Science and Engineering, North Carolina State University, Raleigh, North Carolina 27695-7907
(Received 15 January 1997; revised manuscript received 8 August 1997)

Dielectric and conduction effects in electrorheological (ER) suspensions with non-Ohmic conductivity of the host liquid and with ac applied electric field are investigated. It is found that the conductivity ratio Γ_σ, the non-Ohmic conductivity parameters A and E_c of the host oil, the dielectric constant ratio Γ_ε, and the applied field frequency are important parameters that determine ER response. The effects of these parameters are more complex than in the case of host liquids with simple Ohmic conductivity. If the ac field frequency is high, the conductivity effect disappears; if the frequency is low the dielectric effect disappears. The current density is independent of the frequency below a critical value, but it increases with frequency beyond the critical value. The critical frequency is larger for ER suspensions having non-Ohmic conductivity of the host liquid than with Ohmic conductivity. Good agreement occurs between experimental measurements of the current density and attractive force between particles (including shear yield stress) and predictions by our model. [S1063-651X(97)12511-9]

PACS number(s): 83.80.Gv, 47.50.+d

I. INTRODUCTION

Early studies [1–5] on the interaction force between two adjacent particles in an electrorheological (ER) suspension assumed that both the conductivity and dielectric constant of the materials (particles and host liquid) are independent of the electric field, and thus predicted the interaction force f_a to be proportional to the square of the product of the polarizability β and the applied field E_0, i.e.,

$$f_a \propto (\beta E_0)^2, \tag{1}$$

where

$$\beta = (K_p - K_f)/(K_p + 2K_f) \quad \text{at high frequency ac field} \tag{2a}$$

and

$$\beta = (\sigma_p - \sigma_f)/(\sigma_p + 2\sigma_f) \quad \text{at dc field or low frequency ac field.} \tag{2b}$$

For any other frequency of ac electric field it is suggested that β simply be replaced by the complex polarizability [6–8]

$$\beta^* = (K_p^* - K_f^*)/(K_p^* + 2K_f^*), \tag{3}$$

where the relative complex permittivity $K^* = K - iK''$. K is the real component, $K'' = \sigma/\omega\varepsilon_0$ the loss component, and σ the conductivity; the subscripts p and f refer to the particles and host liquids, respectively.

*On leave from Research Institute of Engineering Mechanics, Dalian University of Technology, Dalian 116024, People's Republic of China.

Recent studies [9–11] on the conductivity of the host liquid show that most oils used in ER suspensions are non-Ohmic, in that the electric field dependence of the conductivity has a form in accord with Onsager's theory [12] for nonpolar liquids. This theory ascribes the increase in conductivity with electric field to an increase of the ionic dissociation constant. Felici, Foulc, and Atten [9] gave the following simplified expression for Onsager's theory for the dependence of the conductivity on electric field:

$$\sigma_f(E) = j/E = \sigma_f(0)[1 - A + A\ \exp(\sqrt{E/E_c})], \tag{4}$$

where j is the current density flowing through the liquid, E the electric field, A a constant, and E_c a characteristic electric field, both depending on the liquid. It has been verified that Eq. (4) is a good approximation of Onsager's theoretical treatment [11].

Using Eq. (4) a number of workers [13–16] developed conduction models for the ER response of suspensions with host oil having non-Ohmic conductivity. These models gave good agreement between predicted ER behavior *with dc field* and that measured. For example, Tang, Wu, and Conrad [13,14] and subsequently Wu and Conrad [15] predicted that the shear yield stress is proportional to $E_0^{1.4-1.6}$ at $E_0 = 0.5 - 5$ kV/mm for zeolite-silicone oil and glass beads-silicone oil suspensions, in accord with experimental results. Futher, Davis and Ginder [16] using a simplified analysis predicted that the shear yield stress of ER fluids is proportional to $E_0^{1.5}$. Davis [17] subsequently gave the same prediction using an integral equation method.

In this paper we develop a general approximate method for predicting the ER response at *any frequency of the electric field for ER suspensions with non-Ohmic conductivity of the host liquid.*

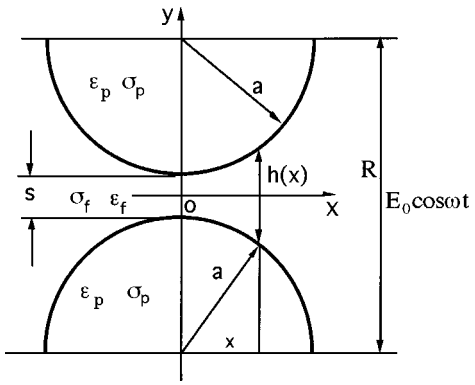

FIG. 1. Geometry of two conducting half spheres immersed in a host liquid. a is the radius of the particles, $h(x)$ is the gap between two particles at location x, $s=h(0)$ is the minimum gap, $E_0=V_0/(2a+s)$ is the magnitude of the applied field, σ is conductivity, and ε is permittivity. The subscripts p and f refer to the particles and the host liquid.

II. BASIC THEORY

Consider a single chain with an infinite number of spherical particles aligned in the direction of the applied electric field and surrounded by a nonpolar liquid. Two half spheres in such a chain are shown in Fig. 1. Assume the applied voltage is

$$V(t)=V_0\cos\omega t=\mathrm{Re}(V_0 e^{i\omega t}), \tag{5}$$

where ω is the annular frequency and t the time. Let E^* denote the complex amplitude of the electric field.

Because we consider a very complex situation where contrasts in both dielectric constant and non-Ohmic conductivity must be taken into, it is too difficult to use an exact theoretical treatment (even a numerical method). Here we use the same assumption proposed by Tang *et al.* [13], i.e., a uniform distribution of the axial field in the particles and host oil. This assumption gave a good estimate for non-Ohmic ER response [9,13–15]. Based on this assumption we have along the y axis in Fig. 1 the following approximate equations:

$$2aE_p^*+sE_f^*=V_0, \tag{6}$$

$$\sigma_p^*E_p^*=\sigma_f^*E_f^*. \tag{7}$$

Equation (6) is a voltage continuity condition and Eq. (7) the current density continuity condition. In the ''contact center'' $(x=0)$, the complex amplitudes of the local electric field in the liquid layer and in the particles are, respectively (see Fig. 1)

$$E_f^*=\frac{\sigma_p^*V_0}{2a\sigma_f^*+s\sigma_p^*}=\frac{(\sigma_p+i\omega\varepsilon_p)V_0}{2a(\sigma_f+i\omega\varepsilon_f)+s(\sigma_p+i\omega\varepsilon_p)}, \tag{8}$$

$$E_p^*=\frac{\sigma_f^*V_0}{2a\sigma_f^*+s\sigma_p^*}=\frac{(\sigma_f+i\omega\varepsilon_f)V_0}{2a(\sigma_f+i\omega\varepsilon_f)+s(\sigma_p+i\omega\varepsilon_p)}, \tag{9}$$

where ε^* is the complex permittivity $\varepsilon^*=\varepsilon+\sigma/i\omega$, σ^* the complex conductivity $\sigma^*=i\omega\varepsilon^*=\sigma+i\omega\varepsilon$, σ and ε the conductivity and permittivity. The subscripts p and f refer to particles and host liquid, respectively. It should be noted that the conductivity of the host liquid is non-Ohmic and is described by Eq. (4) with the electric field E being replaced by the rms value of the local field in the host liquid. Since no exact field dependence of the oil conductivity has been reported for ac field, we will assume that it has the same relation as given for a dc field [Eq. (4)].

The complex amplitude of the current density is

$$j^*=\sigma_p^*E_p^*=\sigma_f^*E_f^*=\frac{\sigma_f^*\sigma_p^*V_0}{2a\sigma_f^*+s\sigma_p^*}. \tag{10}$$

Letting $\Omega=2\pi fK_f\varepsilon_0/\sigma_f(0)$ (where f is the frequency of the applied electric field), $\Gamma_\varepsilon=\varepsilon_p/\varepsilon_f$, $\Gamma_\sigma=\sigma_p/\sigma_f(0)$, $S=s/2a$, we obtain

$$E_f^*=\frac{(1+S)E_0}{\sigma_f^*/\sigma_p^*+S}=\frac{(1+S)E_0}{(\psi+i\Omega)/(\Gamma_\sigma+i\Omega\Gamma_\varepsilon)+S}, \tag{11}$$

where $E_0=V_0/(2a+s)$ is the amplitude of the applied electric field, and

$$\psi=1-A+A\ \exp[|E_f^*|/(\sqrt{2}E_c)]^{1/2}. \tag{12}$$

In the case $x>0$, an equation similar to Eq. (11) is still used to estimate the local electric field distribution between the two adjacent particles. However a and s in Eqs. (8)–(11) should be replaced by $a'=a\sqrt{1-(x/a)^2}$ and $s'=s+2a[1-\sqrt{1-(x/a)^2}]$. The normalized separation S should be replaced by $S'=(S+1)/\sqrt{1-(x/a)^2}-1$.

Having obtained the distribution $E_f^*(x)$ of the complex amplitude of the local electric field, we can get the electric field in the host liquid layer:

$$E_f(x,t)=\mathrm{Re}(E_f^*e^{i\omega t})=\sqrt{2}E(x)\cos[\omega t+\theta_E(\mathbf{x})], \tag{13}$$

where $E(x)=|E_f^*|/\sqrt{2}$ is the rms value of $E_f(x,t)$ and

$$\theta_E=\tan^{-1}\left[\frac{\mathrm{Im}(E_f^*)}{\mathrm{Re}(E_f^*)}\right] \tag{14}$$

is the phase angle shift from the applied field and is a function of the location x and the normalized separation S of the particles. It should be pointed out that the local electric field $E(x)$ is also a function of S. But for simplification we will use $E(x)$ instead of $E(S,x)$.

The complex amplitude of current density is

$$j(x)^*=\sigma_f^*(x)E_f^*(x) \tag{15}$$

and the current density at location x at any time t is

$$j(x,t)=\sqrt{2}j(x)\cos[\omega t+\theta_j(x)], \tag{16}$$

where $j(x)=|j(x)^*|/\sqrt{2}$ is the rms value of $j(x,t)$ and

$$\theta_j=\tan^{-1}\left[\frac{\mathrm{Im}[j(x)^*]}{\mathrm{Re}[j(x)^*]}\right] \tag{17}$$

is the phase angle of the current density shift from the applied electric field, which is a function of the location x and the normalized separation S of the particles. The rms value of the average current density over a chain of particles is

$$J=\left\{\frac{\omega}{2\pi}\int_0^{2\pi/\omega}\left[\frac{1}{\pi a^2}\int_0^a 2\pi x\sqrt{2}j(x)\times\cos[\omega t+\theta_j(x)]dx\right]^2 dt\right\}^{1/2}. \quad (18)$$

If the local field in the liquid layer is much larger than that in the particle, which occurs usually in ER suspensions, the attractive force between two particles is approximated by

$$f_a(t)=\frac{1}{2}\varepsilon_0 K_f\int_0^a 2\pi|E_f(x)^*|^2\cos^2[\omega t+\theta_E(x)]x\ dx$$
$$=\varepsilon_0\pi a^2 K_f E_{\rm rms}^2 F(S,t), \quad (19)$$

where the normalized force $F(S,t)$ is

$$F(S,t)=\int_0^1 2[E(\xi)/E_{\rm rms}]^2\cos^2[\omega t+\theta_E(\xi)]\xi\ d\xi. \quad (20)$$

Here $\xi=x/a$ and $E_{\rm rms}$ is the rms value of the applied electric field. The rms value of the normalized attractive force is

$$F_{\rm rms}=\left(\frac{\psi}{2\pi}\int_0^{2\pi/\omega}F(S,t)^2dt\right)^{1/2} \quad (21a)$$

and the mean value of $F(S,t)$ is

$$F_{\rm mean}=\frac{\omega}{2\pi}\int_0^{2\pi/\omega}F(S,t)dt. \quad (21b)$$

The shear yield stress should be

$$\tau_{E_{\rm rms}}=\varepsilon_f E_{\rm rms}^2\max\left(F_{\rm rms}(\gamma)\frac{\gamma}{\sqrt{1+\gamma^2}}\right) \quad (22a)$$

or

$$\tau_{E_{\rm mean}}=\varepsilon_f E_{\rm rms}^2\max\left(F_{\rm mean}(\gamma)\frac{\gamma}{\sqrt{1+\gamma^2}}\right). \quad (22b)$$

In most experiments, the measuring meters give the rms value of the ac signal, but some meters may give the mean. Since in a real ER fluid there are many chains spanning the two electrodes, Eqs. (19)–(22) should therefore be multiplied by a factor $\frac{3}{2}\phi$ [13–17], where ϕ is the volume fraction of the particles in the ER suspension. If the current passing through both the chain and fluid phases is considered, the current density is

$$J=\left\{\frac{\omega}{2\pi}\int_0^{2\pi/\omega}\left[\frac{1}{a^2}\int_0^a 3\pi\phi x\sqrt{2}j(x)\cos[\omega t+\theta_j(x)]dx+(1-\tfrac{3}{2}\phi)\sqrt{2}j(a)\cos[\omega t+\theta_j(a)]\right]^2 dt\right\}^{1/2} \quad (23)$$

or roughly estimated by omitting the phase angle effects of the current passing through the chains and the pure liquid:

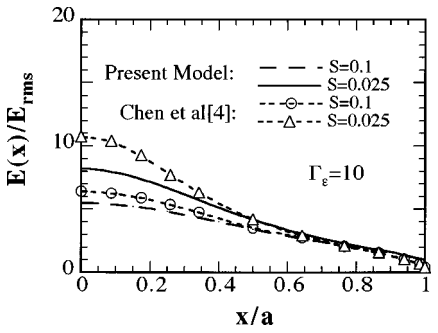

FIG. 2. Comparison of the local field distributions predicted by our model on the midplane between two adjacent particles ($A=0$) and those predicted by Chen *et al.* [4] on the particle surface for an ER chain. See text for assumptions in the calculations.

$$J=\frac{3}{2}\phi\left\{\frac{\omega}{2\pi}\int_0^{2\pi/\omega}\left[\frac{1}{\pi a^2}\int_0^a 2\pi x\sqrt{2}j(x)\times\cos[\omega t+\theta_j(x)]dx\right]^2 dt\right\}^{1/2}+(1-\tfrac{3}{2}\phi)j(a), \quad (24)$$

where $j(a)$ is the current density (rms value) of the pure host liquid under the applied electric field:

$$j(a)=E_{\rm rms}\sqrt{\sigma_f^2+(2\pi f\varepsilon_f)^2}. \quad (25)$$

With dc field $j(a)$ is very small compared to the current density in the chains, but at high ac field it should be considered. It should be pointed out that Eq. (11) is a strong nonlinear complex equation that can be numerically solved by a computer. In all calculations the radius of the particles a is divided into 40 elements.

III. COMPUTED RESULTS

To check the accuracy of our approximate analytical method, Fig. 2 compares the computed local field distribution by Chen *et al.* [4] for an Ohmic ER suspension with our approximate method by taking $A=0$ in Eq. (4). Chen *et al.* did not give the local field distribution in the midplane in the gap between two spheres but only the local field distribution on the sphere surface, so only a rough comparison is given in Fig. 2. In our calculation we take $\Gamma_\varepsilon=10$, $\Gamma_\sigma=0.1$, $\sigma_f=2.4\times10^{-12}$ S/m, $K_f=2.5$, and $f=1000$ Hz, so that the conduction effect disappears. At small separation S, our approximate method gives a slightly lower estimate than Chen *et al.* [4] for the local distribution in the liquid gap near the chain axis (small x), but gives a little higher value than Chen *et al.* far from the chain axis (large x). The reason our method gives a lower estimate for the local field near the axis is mainly due to our assumption mentioned above. Assuming Ohmic conduction of the host liquid the linear numerical solutions [2,18,19] of the field distributions indicate that with small separation S and high Γ_ε (at high frequency ac field) or high Γ_σ (at dc or low frequency ac field), high fields in the gap between spheres are restricted to a small region near the symmetry axis. As a result, much of the potential drop inside a sphere is concentrated into small volumes adjacent to the points of closest approach to other spheres. According to Eq. (7) the local field in the liquid near the sphere surface is high.

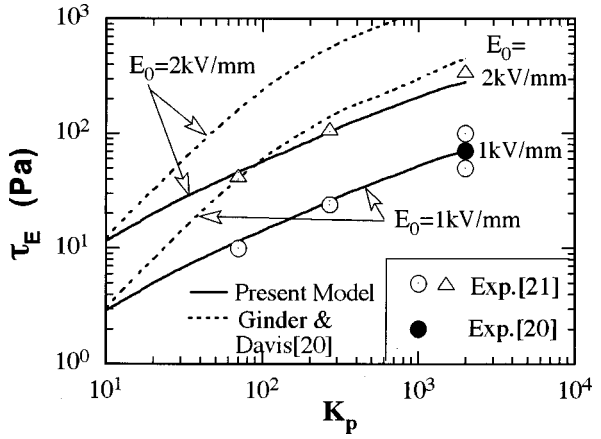

FIG. 3. Comparison of the measured shear yield stress [20,21] and those predicted by the present model (taking $A=0$) and by Ginder and Davis [21] vs the dielectric constant of particles with applied ac field ($f=400$ Hz, $K_f=2$, $\phi=0.2$, $\Gamma_\sigma=10$, and $\sigma_f=10^{-11}$ S/m). The open symbols are the experimental data taken from Garino *et al.* [21] and the solid circle is the experimental value reported by Ginder and Davis [20]. The solid curves are predicted by the present model and the dashed by Ginder and Davis [20].

However, this is a purely theoretical prediction with the important assumption of *Ohmic conductivity*. In practice, the local field in the host oil cannot increase infinitely. On the one hand, the host oil has a breakdown field limit, and on the other, the host oil is usually strongly non-Ohmic at high field

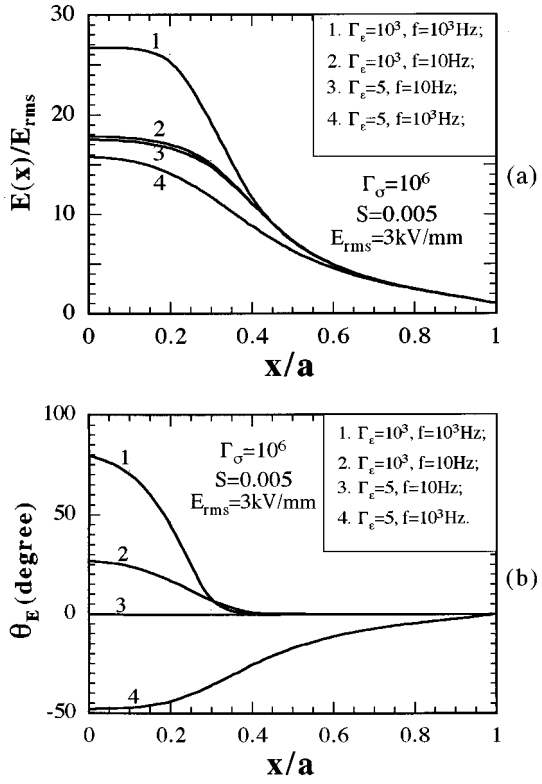

FIG. 4. (a) The local electric field distribution (rms value) in the liquid layer between the two particles and (b) the corresponding phase angle with respect to the applied field ($S=0.005$, i.e., $R/a=2.01$, $\Gamma_\sigma=10^6$). (1) $\Gamma_\varepsilon=10^3$, $f=10^3$ Hz; (2) $\Gamma_\varepsilon=10^3$, $f=10$ Hz; (3) $\Gamma_\varepsilon=5$, $f=10$ Hz; (4) $\Gamma_\varepsilon=5$, $f=10^3$ Hz.

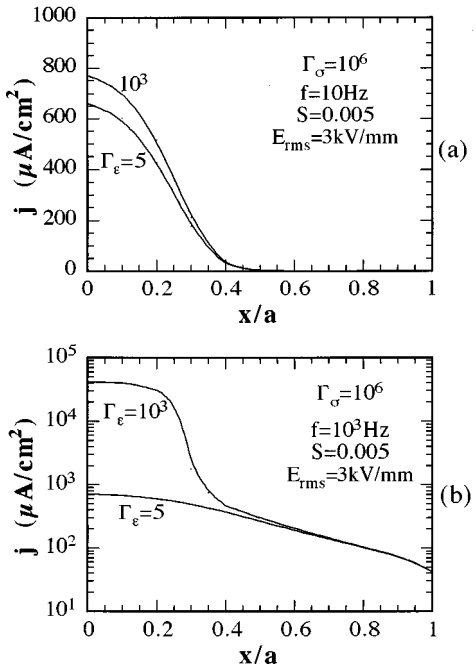

FIG. 5. The local current density distribution (rms value) in the liquid layer between the two particles [$\Gamma_\sigma=10^6$, $S=0.005(R/a=2.01)$, $E_{\rm rms}=3$ kV/mm]: (a) $f=10$ Hz and (b) $f=10^3$ Hz.

[9,10]. For example, Davis [17] using the finite element approach (FEA) predicted the maximum local field in the oil gap is $\sim 1000E_0$ when $\Gamma_\varepsilon=100$ and $S=5\times10^{-4}$ with the assumption of Ohmic conductivity. This means that the maximum local field may reach the order of MV/mm, which is clearly impossible. Finally, for the application of ER fluids, since we are more interested in the shear yield stress (which usually occurs in the range $S=0.02-0.07$ [3]), the so-called exact theoretical calculation of local field in a very small oil gap using the Ohmic conductivity assumption is not very important. This is especially the case when the dielectric constant ratio Γ_ε (at high frequency ac field) or the conductivity ratio Γ_σ (at dc or low frequency ac field) is high.

Figure 3 gives a further comparison of the predicted shear yield stress by our approximate method ($A=0$) and by Ginder and Davis [20]; also given are some experimental data [21]. This indicates that our approximate method gives a more reasonable estimate for the ER shear yield stress than the so-called exact theoretical analysis. When the dielectric constant ratio (or conductivity ratio at dc field) is less than 10 our approximate model gives almost the same estimate as Ginder and Davis [20]. However, Anderson [19] gave at high dielectric ratio a higher predicted yield stress than Ginder and Davis [20] and our model.

In most of the following calculations we will take Dow Corning 200 silicon oil as an example of a host liquid with non-Ohmic conductivity. Experimental measurements [10] give for this oil the non-Ohmic conductivity parameters of Eq. (4): $\sigma_f(0)=2.4\times10^{-12}$ S/m, $A=0.007$, $E_c=0.21$ kV/mm.

Figure 4(a) gives the ratio (rms values) of the local electric field in the liquid gap between two particles to the applied field with different frequencies and for several dielectric and conductivity ratios. The magnitude of the local field

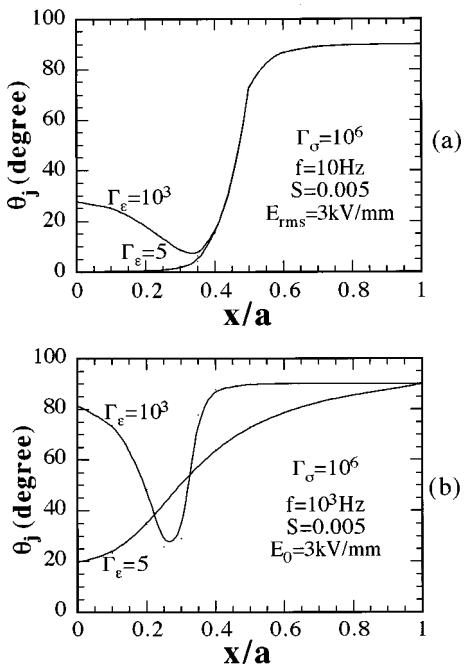

FIG. 6. The phase angle of the electric current with respect to the applied field corresponding to Fig. 5: (a) $f=10$ Hz and (b) $f=10^3$ Hz.

depends on Γ_σ, Γ_ε, $\Omega=2\pi f K_f\varepsilon_0/\sigma_f(0)$, A, and E_c. We cannot easily conclude when the dielectric effect compared to the conduction effect dominates the ER behavior. However, if $\Gamma_\sigma \gg \Gamma_\varepsilon$, the non-Ohmic conduction effect will dominate the ER behavior [here Γ_σ is defined as $\Gamma_\sigma=\sigma_p/\sigma_f(0) \gg \sigma_p/\sigma_f(E)$]. If $\Gamma_\sigma<\Gamma_\varepsilon$, the opposite occurs. Further, a high local electric field occurs mainly in the ''contact zone'' of the two particles, which is also predicted for an Ohmic host oil with ac field [22] and for a non-Ohmic oil with dc field [13–17]. Another characteristic of the local field in a non-Ohmic conduction liquid is that there exists a saturation regime near the contact zone.

Figure 4(b) shows the shifted phase angle of the local electric field from the applied field corresponding to Fig. 4(a). It should be noted that the magnitude of the phase angle does not relate directly to the magnitude of the local electric field.

Figures 5(a) and 5(b) give the rms value of the local current density. The local current density occurs mainly in the

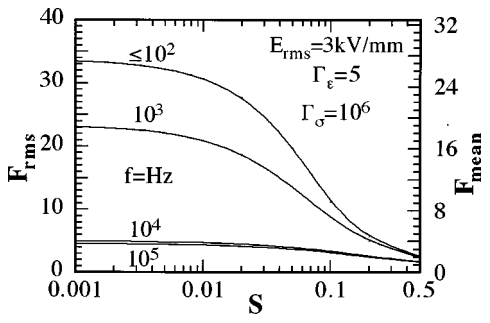

FIG. 7. The normalized attractive force between two particles vs the normalized separation for various frequencies and taking $\Gamma_\varepsilon=5$ and $\Gamma_\sigma=10^6$.

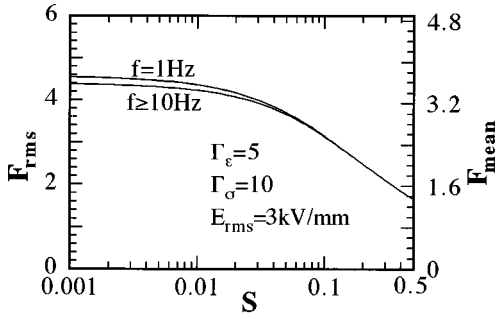

FIG. 8. The normalized attractive force between two particles vs the normalized separation for various frequencies and taking $\Gamma_\varepsilon=5$ and $\Gamma_\sigma=10$.

''contact zone'' at low frequency, but this is not so clear at high frequency (especially with small Γ_ε). Figures 6(a) and 6(b) give the phase angle shift vs x/a. Of interest is that now the corresponding phase angle distribution of the local current density is not the same as that in an Ohmic liquid [see Fig. 2(b) in Ref. [22]]. The strange shape of the phase angle distribution in Figs. 6(a) and 6(b) is due to the non-Ohmic conductivity of the host oil. The phase angle of the current density θ_j is the sum the phase angles of the local field and the complex conductivity of the host liquid. The complex conductivity of the liquid is $\sigma_f^*=i\omega\varepsilon_f^*=\sigma_f(E)+i\omega\varepsilon_f$. In the ''contact zone'' (small x), the conductivity $\sigma_f(E)$ increases to a few orders of magnitude higher than $\sigma_f(E_0)$, which makes the phase angle of the complex conductivity decrease quickly (minimum to 0) with decrease in x. Outside the ''contact zone'' $\sigma_f(E)$ decreases quickly with x to $\sigma_f(E_0)$, which makes the phase angle of the complex conductivity increase rapidly (maximum to 90°). In contrast, the phase angle of the local field decreases rapidly (minimum to 0°) with x [see Fig. 4(b)].

Figures 7 and 8 show, respectively, how the attractive force changes with the normalized separation of the particles and with the frequency of the applied field for a single chain of particles. If $\Gamma_\sigma \gg \Gamma_\varepsilon$, the non-Ohmic conduction effect dominates the ER strength and gives a higher attractive force at low frequency than at high frequency (Fig. 7). If $\Gamma_\sigma<\Gamma_\varepsilon$, but they are of the same order of magnitude, little difference is observed for different frequencies (Fig. 8).

Figure 9 gives the rms values of the attractive force versus the normalized separation when $\Gamma_\sigma=10$ and $\Gamma_\varepsilon=10^3$. A stronger ER response occurs at high frequency than at low frequency. It should be pointed out that in the case of non-Ohmic conductivity of the host oil the rms value of the attractive force $F_{\rm rms}$ is not equal to $\sqrt{3/2}F_{\rm mean}$ especially at high Γ_ε. Usually $F_{\rm rms}=(1.1-\sqrt{3/2})F_{\rm mean}$. The reason the curves in Figs. 7, 8, and 9 tend to decrease to the same value as S becomes large is that the non-Ohmic conductivity effect disappears and the frequency has little effect on the ER response. The point-dipole approximation gives $F_{\rm rms}=0.3$ when $S=0.5$ and $\Gamma_\varepsilon=1000$ compared to $F_{\rm rms}\approx 2$ predicted by our model.

Figures 10 and 11 show the average current density along a chain for different magnitudes of Γ_σ and Γ_ε. The current density in general has a larger value at high frequency than at low frequency. When $S<0.1$ the current density shows only little change with separation of the particles.

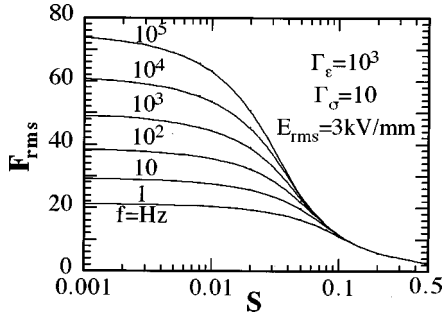

FIG. 9. The normalized attractive force (rms value) between two particles vs the normalized separation for various frequencies and taking $\Gamma_\varepsilon=10^3$ and $\Gamma_\sigma=10$.

Figures 12(a) and 12(b) give the shear yield stress and current density versus the frequency for different values of Γ_σ and Γ_ε. If $\Gamma_\sigma \gg \Gamma_\varepsilon$, a higher shear yield stress occurs at low than at high frequency; if $\Gamma_\sigma < \Gamma_\varepsilon$, the opposite occurs. The rms value of the shear yield stress is about 1.2 times the mean value, which is slightly different from the attractive force. Of interest is that, if the dielectric effect is larger than the conductivity effect, the transition regime from the conductivity domain to the dielectric domain is larger than in the case of Ohmic conductivity of the host liquid [22]. The reason for this is that with an increase in frequency, the dielectric influence increases; i.e., the local field increases. However, due to the non-Ohmic conductivity of the host liquid, its conductivity increases with the increase in the local field. Obviously, the stronger the non-Ohmic character of the host fluid, the less will be the increase in local field. However, if the dielectric effect is smaller than the conductivity effect [Fig. 12(a), case 1], the transition regime is of the same order as that for Ohmic conductivity. The reason curves 2, 3, and 4 converge in Figs. 12(a) and 12(b) at a high frequency is that these three curves have the same dielectric constant ratio but have different conductivity ratios.

Figure 13(a) shows the shear yield stress (rms value) dependence on the applied field when the dielectric ratio is smaller than the conductivity ratio ($\Gamma_\varepsilon \ll \Gamma_\sigma$). The ER response at low frequency ($f \leqslant 10^2$ Hz) is stronger than that at high frequency and has a field dependence of $E_{\rm rms}^{1.5}$. At high frequency ($f \geqslant 10^3$ Hz) the shear yield stress has a field dependence of $E_{\rm rms}^2$. It is interesting that, although $f=10^3$ Hz is in the transition regime [see Fig. 13(a)] the shear yield stress still shows a field dependence of $E_{\rm rms}^2$. In contrast to

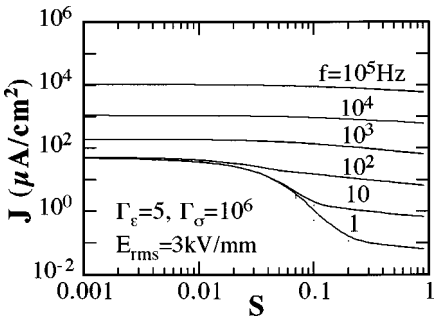

FIG. 10. The average current density of a single chain of particles vs the normalized separation for various frequencies. $\Gamma_\varepsilon=5$, $\Gamma_\sigma=10^6$, and $E_{\rm rms}=3$ kV/mm.

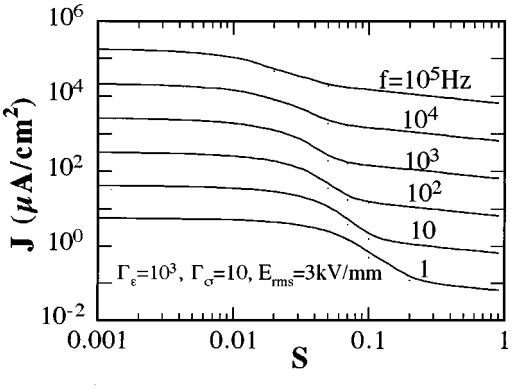

FIG. 11. The average current density of a single chain of particles vs the normalized separation for various frequencies. $\Gamma_\varepsilon=10^3$, $\Gamma_\sigma=10$, and $E_{\rm rms}=3$ kV/mm.

Fig. 13(a), Fig. 13(b) gives the case when the dielectric effect is larger than the non-Ohmic conductivity effect, even though $\Gamma_\sigma=\sigma_p/\sigma_f(0)>\Gamma_\varepsilon=\varepsilon_p/\varepsilon_f$. This gives a weaker ER response at low frequency than that at high frequency and the shear yield stress has a field dependence of $E_{\rm rms}^{1.51}$, $E_{\rm rms}^{1.53}$, and $E_{\rm rms}^{1.54}$ for the frequency $f=0$, 50, and 10^3 Hz, respectively.

IV. COMPARISON OF THEORY WITH EXPERIMENT

Figure 14 compares the predicted value of the attractive force (taking $S=10^{-5}$) and that measured by Boissy, Foulc,

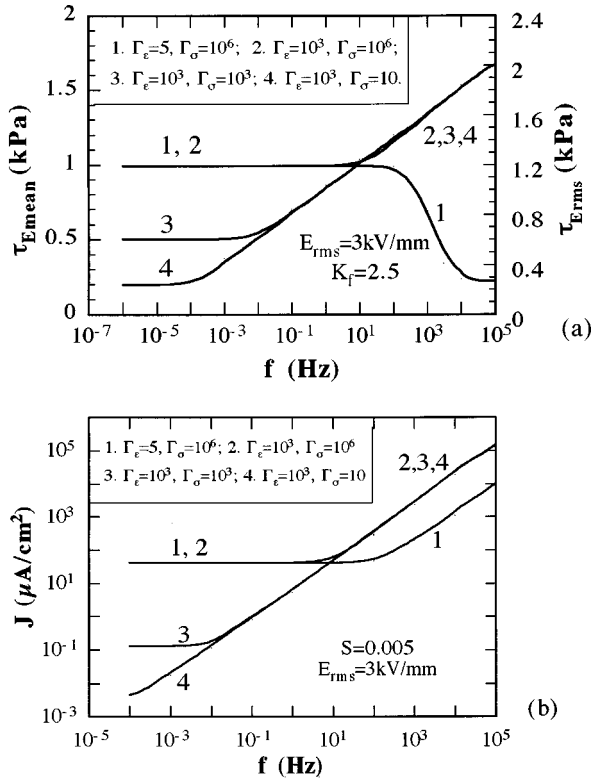

FIG. 12. The ER response in the transition region, conductivity domain, and dielectric domain for a single chain of particles ($S=0.005$, $E_{\rm rms}=3$ kV/mm): (a) the shear yield stress and (b) the average current density. (1) $\Gamma_\varepsilon=5$, $\Gamma_\sigma=10^6$; (2) $\Gamma_\varepsilon=10^3$, $\Gamma_\sigma=10^6$; (3) $\Gamma_\varepsilon=\Gamma_\sigma=10^3$; (4) $\Gamma_\varepsilon=10^3$, $\Gamma_\sigma=10$.

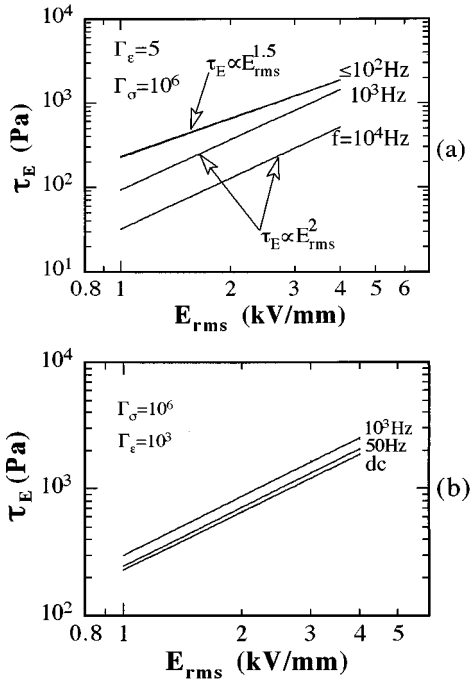

FIG. 13. The shear yield stress (rms value) dependence on the applied field at various frequencies for a single chain of particles: (a) $\Gamma_\varepsilon=5$, $\Gamma_\sigma=10^6$ and (b) $\Gamma_\varepsilon=10^3$, $\Gamma_\sigma=10^6$.

and Atten [23]. The radius of the two half-sphere particles is 7 mm (the distance between the electrodes is 14 mm). The conductivity of the particles given in Ref. [23] is $\sigma_p=1.7\times10^{-8}$ S/m. The non-Ohmic conductivity parameters of the oil are obtained by fitting the experimental data (curve 1 in Fig. 6 of Ref. [24]) to Eq. (4). They are $\sigma_f(0)=3\times10^{-13}$ S/m, $A=1.35$, and $E_c=1.49$ kV/mm. The dielectric constant of the oil is $K_f=2.2$. The dielectric constant of the particles decreases with the frequency [23], i.e., when the frequency $f=10$, 50, and 1000 Hz, the dielectric constant of the particles is $K_p=34$, 24, and 18, respectively. Evident in Fig. 14 is that the attractive force predicted by the present model is in good agreement with that measured. The reason the measured force at low field and high frequency is slightly smaller than predicted is probably that the force is too small to be measured accurately [25].

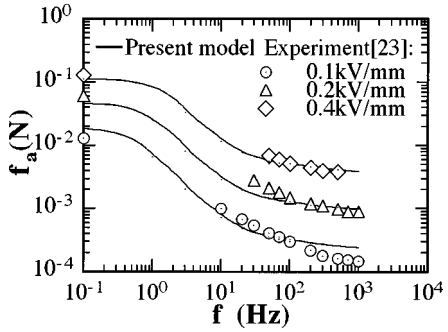

FIG. 14. Comparison of the frequency dependence of the predicted attractive force (rms value) between two polymer particles immersed in mineral oil (Elf TF50) with that measured by Boissy, Foulc, and Atten [23] (experimental: open symbols; theoretical: solid curves). Radius of the particles $a=7$ mm, $S=10^{-5}$.

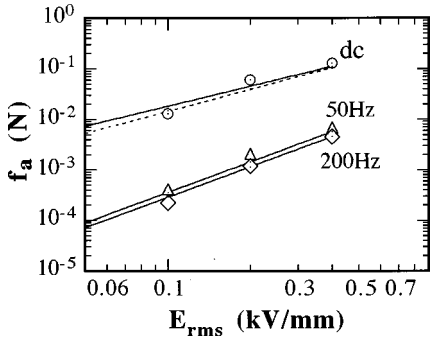

FIG. 15. Comparison of the electric field dependence of the predicted attractive force (rms value) between two polymer particles immersed in mineral oil (Elf TF50) with those measured by Boissy, Foulc, and Atten [23] (experimental: open symbols; theoretical: solid curves for $S=10^{-5}$ and dashed curves for $S=0.001$) Radius of the particles $a=7$ mm. Note that when $f=50$ and 200 Hz the solid curves for $S=10^{-5}$ and the dashed curves for $S=0.001$ come together.

Figure 15 gives the dependence of the attractive force on the applied field (again taking $S=10^{-5}$). At ac field frequencies $f=50$ and 200 Hz, our model predicts that the attractive force is proportional to $E_{\rm rms}^2$, in good agreement with experiment. With dc field the predicted attractive force is proportional to $E_{\rm rms}^{1.3}$ ($S=10^{-5}$) compared to the experimental $F_{\rm rms}\propto E_{\rm rms}^{1.6}$. If we take $S=10^{-2}$ our model predicts that $F_{\rm rms}\propto E_{\rm rms}^{1.45}$ (dashed line in Fig. 15), which is in better agreement with experiment. With ac fields the predicted force has no dependence on S in this range of particle separation. The reason the dependence of the attractive force on dc field varies only slightly with S is that at high field saturation of the local field occurs for a large range of S. At low field, however, only in a small range of S does saturation occur. Hence, increasing S leads to a slight increase in the attractive force (see the dashed line in Fig. 15). A detailed investigation of field saturation is given in Refs. [9–11,15].

Figure 16 compares the predicted gain-frequency characteristic of the system of two polymer particles in mineral oil

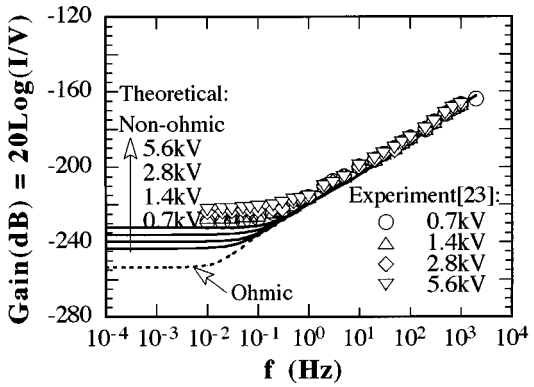

FIG. 16. Comparison of the predicted gain of two polymer particles immersed in mineral oil vs the frequency with that measured by Boissy, Foulc, and Atten [23] (experimental: open symbols; theoretical: solid curves for non-Ohmic conductivity and dashed curve for Ohmic conductivity). Radius of the particles $a=7$ mm, $S=0.10^{-5}$. Gain is defined as $\ln(I/V)$, where I is the output current and V the applied field.

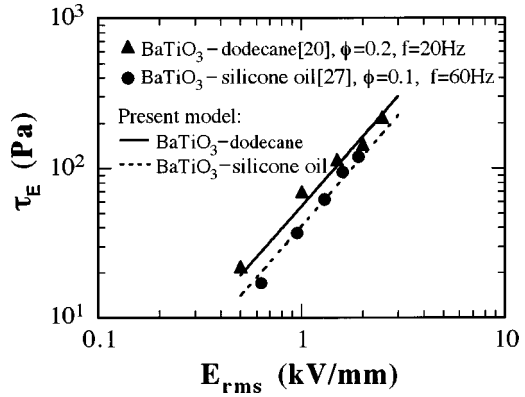

FIG. 17. Comparison of the predicted shear yield stress (rms value) with that measured by Miller, Randall, and Bhalla [27] for $BaTiO_3$–silicone oil suspension [$f=60$ Hz and $\phi=0.1$, $K_f=2.8$, $K_p=2000$, $\sigma_p=10^{-10}$ S/m, $\sigma_f(0)=2.4\times10^{-12}$ S/m, $A=0.007$, $E_c=0.21$ kV/mm] and by Ginder and Davis [20] for $BaTiO_3$–dodecane suspension [$f=20$ Hz and $\phi=0.2$, $K_f=2.0$, $K_p=2000$, $\sigma_p=10^{-10}$ S/m, $\sigma_f(0)=2.4\times10^{-12}$ S/m, $A=0.007$, $E_c=0.21$ kV/mm].

and that measured, where gain$=\ln(I/V)$, I is the measured output current and V the applied voltage (rms value). At high frequency the predicted value is in good agreement with experiment [23]. At low frequency, although the predicted value is smaller than that measured, the general trend of the gain is to increase with the applied voltage, similar to the experiments. The possible reasons for the difference at low frequency [25,26] are (a) experimental error and (b) the conductivity $\sigma_f(0)=3\times10^{-13}$ S/m of the oil at low field used in the experiment is slightly higher than given in Ref. [23]. If we take $\sigma_f(0)=10^{-12}$ S/m, the predicted gain is in good agreement with experiment over the entire frequency range.

Figure 17 compares the dependence of the shear yield stress on the ac applied field predicted by the present model for $BaTiO_3$–silicone oil and $BaTiO_3$-dodecane suspensions and that measured by Miller *et al.* [27] and by Ginder and Davis [20]. Again, there is good agreement between the predicted and measured values for both suspensions.

V. DISCUSSION

This paper investigates combined effects of dielectric and conduction in the ER response of suspensions with ac field, assuming that the conductivity of the host liquid is non-Ohmic. The derived model predicts that the shear yield stress of an ER fluid is proportional to the square of the applied electric field in the dielectric domain (i.e., at high frequency), and to about the $\frac{3}{2}$ power in the conductivity domain (dc or low frequency ac field). The agreement with experiment is better than when the conductivity of host liquid is assumed to be Ohmic [22].

Whittle *et al.* [28] included a Debye-type relation in their expression of the complex dielectric constant and compared their experimental results of the pressure drop in an ER valve versus frequency with the real and imaginary components of the calculated $\beta^*(\omega)^2$. Although we did not include the Debye effect in our calculations, it can be easily included. However, in practice the frequency of the applied field is usually $<10^4$ Hz and only a few materials exhibit a Debye frequency within this range [29].

VI. SUMMARY AND CONCLUSIONS

Combined dielectric and conduction effects in ER fluids with non-Ohmic conductivity of the host liquid were investigated for ac electric field. The following is a summary of the results obtained and conclusions derived therefrom:

(1) Important parameters affecting ER behavior are the conductivity ratio at low field $\Gamma_\sigma=\sigma_p/\sigma_f(0)$, the dielectric permittivity ratio $\Gamma_\varepsilon=\varepsilon_p/\varepsilon_f$, the normalized frequency $\Omega=2\pi f\varepsilon_0 K_f/\sigma_f(0)$, and the non-Ohmic conductivity parameters A and E_c of the host oil. If $\Gamma_\sigma\gg\Gamma_\varepsilon$, the ER fluid has a high shear yield stress at low frequency; if $\Gamma_\sigma<\Gamma_\varepsilon$, the opposite occurs. The combined effect of these parameters on the ER behavior is more complicated than in the case of simply Ohmic conductivity of the host liquid.

(2) In the conductivity domain (dc or low frequency ac electric field), the shear yield stress is proportional to $E_{\rm rms}^{1.5}$; in the dielectric domain (high frequency ac field) the shear yield stress is proportional to $E_{\rm rms}^2$. In the transition regime, the situation is complex. If the dielectric ratio is greater than the conductivity ratio, the shear yield stress exhibits a $\sim E_{\rm rms}^{1.5}$ dependence on the applied field over most of the transition regime. However, if the dielectric ratio is smaller than the conduction ratio, the shear yield stress exhibits a $E_{\rm rms}^2$ dependence over most of the transition regime.

(3) The current density of an ER fluid is proportional to $\sigma_f(0)E_{\rm rms}$. In the conductivity domain (low frequency), the current density is independent of the frequency. However, in the dielectric domain and the transition regime, the current density increases with frequency at slightly less than the first power (i.e., roughly proportional).

(4) Good agreement occurs between the predicted and measured attractive force of two nearly touching polymer spheres immersed in mineral oil and between the predicted and measured shear yield stress of a $BaTiO_3$-silicone oil suspension. Also, good agreement occurs between the predicted current density and that measured for the two polymer spheres in mineral oil.

ACKNOWLEDGMENTS

This research was sponsored jointly by the NSF Engineering Directorate under Grant CTS-9313897 with Dr. M. C. Roco as technical monitor and by the NCSU/Industry Consortium on ER Fluids with membership by Bridgestone, Ford, Paar-Physica, and Texaco. The authors acknowledge helpful discussions with Dr. C. Boissy. Dr. C. W. Wu wishes to express his appreciation to the China NSF and BSDF for their support during his visit to NCSU.

[1] A. P. Gast and C. F. Zukoski, Adv. Colloid Interface Sci. **30**, 153 (1989).
[2] R. A. Anderson, in *Proceedings of the 3th International Conference on ER Fluids*, edited by R. Tao and G. D. Roy (World Scientific, Singapore, 1992), pp. 81–92.
[3] D. J. Klingenberg and C. F. Zukoski, Langmuir **6**, 15 (1990).
[4] Y. Chen, A. F. Sprecher, and H. Conrad, J. Appl. Phys. **70**, 6796 (1991).
[5] L. C. Davis, J. Appl. Phys. **72**, 1334 (1992).
[6] H. Conrad and Y. Chen, in *Progress in Electrorheology*, edited by K. O. Havelka and F. E. Filisko (Plenum Press, New York, 1995), pp. 55–86.
[7] Y. D. Kim and D. J. Klingenberg, in *Progress in Electrorheology*, edited by K. O. Havelka and F. E. Filisko (Plenum Press, New York, 1995), pp. 115–130.
[8] R. M. Webber, in *Progress in Electrorheology* (Ref. [7]), pp. 171–184.
[9] N. Felici, J. N. Foulc, and P. Atten, in *Proceedings of the 4th International Conference on ER Fluids*, edited by R. Tao and G. D. Roy (World Scientific, Singapore, 1994), pp. 139–152.
[10] C. W. Wu, Y. Chen, X. Tang, and H. Conrad, Int. J. Mod. Phys. B **10**, 3315 (1996).
[11] C. W. Wu, Y. Chen, and H. Conrad, in *Rheology and Fluid Mechanics of Nonlinear Masterials*, Applied Mechanics Division, Vol. 217, edited by D. A. Siginer and S. G. Advani (ASME, New York, 1996), pp. 267–276.
[12] L. Onsager, J. Chem. Phys. **2**, 599 (1934).
[13] X. Tang, C. W. Wu, and H. Conrad, J. Rheol. **39**, 1059 (1995).
[14] X. Tang, C. W. Wu, and H. Conrad, J. Appl. Phys. **78**, 4183 (1995).
[15] C. W. Wu and H. Conrad, J. Phys. D **29**, 3147 (1996).
[16] L. C. Davis and J. M. Ginder, in *Progress in Electrorheology*, edited by K. O. Havelka and F. E. Filisko (Plenum Press, New York, 1995), pp. 107–114.
[17] L. C. Davis, J. Appl. Phys. **81**, 1985 (1997).
[18] M. J. Chrzan and J. P. Coulter, Int. J. Mod. Phys. B **6**, 2651 (1992).
[19] R. A. Anderson, Langmuir **10**, 2917 (1994).
[20] J. M. Ginder and L. C. Davis, in *Proceedings of the 4th International Conference on ER Fluids*, edited by R. Tao and G. D. Roy (World Scientific, Singapore, 1994), pp. 267–282.
[21] T. Garino, D. Adolf, and B. Hance, in *Proceedings of the 3rd International Conference on ER Fluids*, edited by R. Tao (World Scientific, Singapore, 1992), pp. 167–174.
[22] C. W. Wu and H. Conrad, J. Phys. D **30**, 2634 (1997).
[23] C. Boissy, J. N. Foulc, and P. Atten, in *Proceedings of the 4th International Conference on ER Fluids* (Ref. [20]), pp. 453–462.
[24] P. Atten, J. N. Foulc, and H. Benqassmi, in *Progress in Electrorheology* (Ref. [16]), pp. 231–244.
[25] C. Boissy (private communication).
[26] C. Boissy, P. Atten, and J. N. Foulc, in *Proceedings of the 5th International Conference on ER Fluids, MR Suspension and Associated Technology*, edited by W. A. Bullough (World Scientific, Singapore, 1996), pp. 756–763.
[27] D. V. Miller, C. Randall, and A. S. Bhalla, Ferroelectr. Lett. Sect. **15**, 141 (1993).
[28] M. Whittle, W. A. Bullough, D. J. Peel, and R. Firoozian, Phys. Rev. E **49**, 5249 (1994).
[29] C. J. F. Bottcher and P. Bordewijk, *Theory of Electric Polarization: Volume II Dielectric in Time-Dependent Fields* (Elsevier Scientific Publishing Co., Amsterdam, 1978).